Biochemistry and Biophysics Reports 9 (2017) 51–60

Contents lists available at ScienceDirect

Biochemistry and Biophysics Reports

journal homepage: www.elsevier.com/locate/bbrep

De novo protein sequencing, humanization and in vitro effects of an antihuman CD34 mouse monoclonal antibody

Chia-Yu Fan[a,b], Sheng-Yu Huang[c], Min-Yuan Chou[b,*], Ping-Chiang Lyu[a,*]

[a] Institute of Bioinformatics and Structural Biology & Department of Life Science, National Tsing Hua University, Hsinchu, Taiwan
[b] Biomedical Technology and Device Research Laboratories, Industrial Technology Research Institute, Hsinchu, Taiwan
[c] Mithra Biotechnology Inc., New Taipei City, Taiwan

ARTICLE INFO

Keywords:
Monoclonal antibody
De novo sequencing
Humanization
CD34
Antiangiogenic therapy

ABSTRACT

QBEND/10 is a mouse immunoglobulin lambda-chain monoclonal antibody with strict specificity against human hematopoietic progenitor cell antigen CD34. Our in vitro study showed that QBEND/10 impairs the tube formation of human umbilical vein endothelial cells (HUVECs), suggesting that the antibody may be of potential benefit in blocking tumor angiogenesis. We provided a de novo protein sequencing method through tandem mass spectrometry to identify the amino acid sequences in the variable heavy and light chains of QBEND/10. To reduce immunogenicity for clinical applications, QBEND/10 was further humanized using the resurfacing approach. We demonstrate that the de novo sequenced and humanized QBEND/10 retains the biological functions of the parental mouse counterpart, including the binding kinetics to CD34 and blockage of the tube formation of the HUVECs.

1. Introduction

The CD34 protein belongs to the family of single-pass transmembrane sialomucin proteins, with an apparent molecular mass (Mr) of approximately 115 kD [1,2]. Cells with the CD34 surface protein could be found in the bone marrow, umbilical cord blood and peripheral blood as hematopoietic progenitor cells and vascular endothelial cells [3–7]. $CD34^{+}$ hematopoietic cells enriched from bone marrows have traditionally been used clinically in patients after radiation therapy or chemotherapy [8,9]. In previous studies, it was revealed that $CD34^{-/-}$ mice start to exhibit an abnormal vessel morphology when they are triggered by disease models, such as autoimmune arthritis [10], tumor angiogenesis [11], and oxygen-induced retinopathy [12]. Furthermore, CD34 expressed on human umbilical vascular endothelial cells (HUVECs) show the angiogenic tip cell phenotype [13]. Therefore, anti-CD34 should be considered when developing antiangiogenic therapy.

Angiogenesis is a physiological process related to the sprouting and growth of new vessels from an existing vasculature. Angiogenesis is the predominant pathway for neovessel growth in malignancy [14]; therefore, the process is called tumor angiogenesis. In 1971, Folkman first proposed the hypothesis that tumor growth is angiogenesis dependent [15], according to which angiogenesis presents unique opportunities for therapeutic intervention in cancer treatment. During vascular network expansion, sprouting angiogenesis requires a subset of highly specialized endothelial cells, namely tip cells. The tip cells start migrating and existing at the leading front of the growing vessels to guide migration toward a source of angiogenic growth factors, such as vascular endothelial growth factor (VEGF) [16–20], platelet-derived growth factor [21], placental growth factor [19,20,22], fibroblast growth factor-2 [18,23], interleukin-8 [24,25], transforming growth factor-beta [26–28], and angiopoietins [29,30].

Most monoclonal antibodies (mAbs) originate from mice; therefore, a human antimouse [31] or antichimeric [32] antibody might be evoked when mouse antibodies are applied in human therapy. To circumvent such an adverse immune response, mouse antibodies must be humanized for clinical applications [33]. Antibody humanization involves maintaining the specificity and affinity of the parental nonhuman antibody and designing an antibody molecule to reduce the immunogenicity to the greatest extent possible.

QBEND/10 is a mouse mAb against CD34; it reacts with the class II epitope of CD34 [34]. The CliniMACS CD34 reagent system (Miltenyi Biotec, Bergisch Gladbach, Germany) is a clinically approved device for selecting hematopoietic stem cells from donor apheresis. CliniMACS uses mouse QBEND/10 directly conjugated to an iron oxide particle. Notably, in our current in vitro study, mouse QBEND/10 impaired the tube formation of HUVECs. To address the therapeutic potential of QBEND/10, we used de novo protein sequencing and antibody

* Corresponding authors.
E-mail addresses: minyuanc@itri.org.tw (M.-Y. Chou), pclyu@mx.nthu.edu.tw (P.-C. Lyu).

http://dx.doi.org/10.1016/j.bbrep.2016.11.006
Received 10 July 2016; Received in revised form 25 October 2016; Accepted 15 November 2016
Available online 18 November 2016

humanization technology as well as analyzed the effects of humanized QBEND/10 on angiogenesis in vitro by inhibiting the tube formation of HUVECs.

2. Materials and methods

2.1. Materials

Mouse QBEND/10 was purchased from AbD Serotec. Ammonium bicarbonate, dithiolthreitol (DTT), iodoacetamide (IAM), formic acid (FA), thermolysin, and subtilisin were purchased from Sigma–Aldrich. Urea and acetonitrile (ACN) were purchased from J.T Baker. Trypsin and chymotrypsin were purchased from Promega. Endoproteinase Glu-C (Glu-C) and peptide N-glycosidase F (PNGase F) were purchased from New England BioLabs and Roche, respectively. Furthermore, 4–12% and 4–20% NuPAGE Bis-Tris polyacrylamide gels were purchased from Invitrogen. Amicon Ultra centrifugal filters (molecular weight cut-off, 100 kDa) were purchased from Millipore.

2.2. Enzymatic digestion and deglycosylation of QBEND/10

Mouse QBEND/10 was first processed for detergent removal and buffer exchange into 50 mM ammonium bicarbonate buffer solution by using the centrifugal filters. QBEND/10 was subsequently denatured using 6 M urea, reduced with 10 mM DTT at 37 °C for 1 h and alkylated using 50 mM IAM for 30 min in the dark at room temperature (RT). The resulting protein was individually digested with trypsin, Glu-C, thermolysin, chymotrypsin, and subtilisin at 37 °C for 18 h (protein:enzyme=20:1). One aliquot of the trypsin digest was added to Glu-C for 20-h digestion at 37 °C. Thereafter, PNGase F was added for the deglycosylation reaction. The samples were subsequently diluted and acidified to 0.1% FA for liquid chromatography (LC)–mass spectrometry (MS) analysis.

2.3. In-gel tryptic digestion

In a parallel experiment, a mini gel (8 cm×8 cm, 4–20% NuPAGE Bis-Tris polyacrylamide gel) was used for separation through sodium dodecyl sulfate polyacrylamide gel electrophoresis (SDS-PAGE), followed by Coomassie Brilliant Blue R-250 staining. Two bands containing proteins with an apparent Mr of approximately 25 and 50 kDa were excised from the gel, washed, in-gel reduced, alkylated, and digested overnight with trypsin.

2.4. Liquid chromatography–tandem mass spectrometry analysis

The samples were analyzed with a Q Exactive mass spectrometer (Thermo Scientific) coupled with an Ultimate 3000 RSLC system (Dionex). LC was performed using the C18 column (Acclaim PepMap RSLC; 75 μm×150 mm, 2 μm, 100 Å) with a linear gradient of 1–25% of mobile phase B (mobile phase A: 5% ACN/0.1% FA; mobile phase B: 95% ACN/0.1% FA) for 40 min, 25–60% of mobile phase B for 3 min, and 60–80% of mobile B for 2 min for a total separation time of 70 min. A full MS scan was obtained in the range of m/z 350–2000, and the 10 most intense ions from the scan were subjected to fragmentation for MS/MS spectra. Raw data were processed into peak lists by using Proteome Discoverer 1.3 for a Mascot database search.

2.5. Database search and de novo sequencing

A customized database was prepared by collecting the sequences of immunoglobulins (IgGs) from the National Center for Biotechnology Information (NCBI) database. The database was searched using Mascot version 2.4.0. Carbamidomethylation was selected as the fixed modification, and deamidation (NQ), oxidation (M), and pyroglutamate (N-term Q) were included as variable modifications. Up to five missed cleavages were allowed for each enzyme digestion and ± 5 ppm and ± 0.02 Da were used as the mass tolerance window for parent and fragment ions, respectively. Furthermore, an error-tolerant search was performed, in which all modifications and sequence variations were considered. The MS/MS spectra with high intensities were manually sequenced if they had not been identified using Mascot. A customized computational algorithm was constructed to categorize the observed peptides as a heavy or light chain and then align the peptides into a complete sequence. The results were specified in Mascot as a new database for protein identification and an error-tolerant search. The process was repeated iteratively until the protein sequence with the highest possible score was obtained. All MS/MS spectra in this study were manually validated to assure their quality.

2.6. Molecular modeling

Molecular modeling of the variable fragment (Fv) of mouse QBEND/10 was performed using the Prediction of Immunoglobulin Structure (PIGS; http://www.biocomputing.it/pigs) [35,36] Web server through single sequence submission. The structural model of the mouse QBEND/10 Fv region was generated from the corresponding amino acid sequence by using PIGS with default settings. The most suitable heavy and light chain templates were selected from the 20 templates displayed. The Protein Data Bank (PDB) codes 2GKI_H [37] and 2QHR_L [38], exhibiting 86.67% and 94.92% sequence similarity with mouse QBEND/10 VH and VL, respectively, were used to model the three-dimensional (3D) structure of mouse QBEND/10. For the automated construction of the 3D structure of the Fv region of mouse QBEND/10, a canonical loop grafting approach was used for CDRs L1–L3 and H1–H3. The position of the conserved amino acid side chains was maintained, whereas the nonconserved amino acid side chains were modeled using SCWRL 4.0 [39]. Energy minimization was performed using the Swiss-PdbViewer application [40].

2.7. QBEND/10 humanizaiton

Mouse QBEND/10 was humanized using the resurfacing approach [41]. The variable heavy and light (VH and VL, respectively) chains and CDRs were numbered and identified according to the method proposed by Kabat [42]. First, the generated Fv model of mouse QBEND/10 was used to identify surface accessible residues by using Swiss-PdbViewer [40], with the threshold set at 30% [43]. Second, the sequence of mouse QBEND/10 VH and VL chains was searched using NCBI IgBLAST against the human IgG germline database (http://www.ncbi.nlm.nih.gov/igblast/). Human germline V sequences with the highest identity to mouse VH and VL regions were used. The J region for the heavy and light chains was selected from the most identical human consensus sequence. Third, these crucial surface residues of the framework regions were manually exchanged with those from the selected human IgG germline sequence. These side chains were rotated manually to evaluate stable side chain conformation and were subsequently subjected to energy minimization using Swiss-PdbViewer. Finally, the sequence composition for the Fv region of the resurfaced QBEND/10 was assembled. Two resulting models, mouse and humanized QBEND/10, were analyzed, visualized, and superimposed with Swiss-PdbViewer [40]. On the basis of the superimposition result, structural changes in the CDRs were determined.

2.8. Recombinant plasmid construction

The DNA sequences of QBEND/10 VH and VL were separately synthesized using GenScript (GenScript USA Inc., Piscataway, NJ, USA). The coding region of the heavy chain is composed of an N-terminal QBEND/10 VH and a C-terminal human IgG1 constant region (CH1, hinge, CH2, and CH3) nucleotide sequence. This synthetic gene was prepared through overlapping polymerase chain reaction (PCR). The PCR product flanked with *Eco*RV and *Bam*HI sites was cloned into the expression vector pSecTag2/Hygro (Thermo Fisher Scientific, Waltham, MA, USA) at the same sites. The entire heavy chain DNA of QBEND/10 was cloned in-frame with the N-terminal mouse Ig kappa-chain V-J2-C signal peptide of the pSecTag2/Hygro expression vector for secretion. The coding region of the light chain was composed of an N-terminal QBEND/10 VL and C-terminal lambda light chain constant region nucleotide sequence. This synthetic gene was prepared through overlapping PCR. The PCR product was cloned into the expression vector pcDNA3.3–TOPO TA (Thermo Fisher Scientific). The entire VL DNA segment of QBEND/10 was also cloned in-frame with the V-J2-C signal peptide for secretion.

2.9. Antibody expression and purification

Recombinant QBEND/10 antibodies were obtained through a stable cotransfection of expression constructs in mouse myeloma NS0 cells (European Collection of Animal Cell Cultures, Wiltshire, UK) by using Effectene (QIAGEN Inc., Valencia, CA, USA) according to the manufacturer's instructions. After selection with 400 μg/mL hygromycin B (Thermo Fisher Scientific) and 800 μg/mL G418 (Thermo Fisher Scientific) for 4 weeks, a stable clone was cultured in a shaker flask at an initial seeding density of 5×10E5 cells/mL in the chemically defined medium HyClone CDM4NS0 (Hyclone, GE Healthcare, South Logan, UT, USA) containing 2% fetal bovine serum (FBS). The culture was maintained at 130 rpm for 5 days at 37 °C. The recombinant antibodies were purified from the supernatant by using a human-IgG affinity column (IgSelect; GE Healthcare).

2.10. SDS-PAGE

SDS-PAGE was performed using a 4–12% NuPAGE Bis-Tris polyacrylamide gel with 3-morpholinopropanesulfonic acid (MOPS) as the running buffer (Thermo Fisher Scientific). The proteins were stained with Coomassie brilliant blue R-250.

2.11. ELISA

The protein concentrations were estimated using the procedure reported by Bradford [44]. In brief, a Nunc™ MaxiSorp 96-well plate (Thermo Fisher Scientific) was coated with the human CD34 protein (Fc tag; Sino Biological Incorporation, Beijing, China) in a volume of 50 μL at a concentration of 5 μg/mL and incubated at 4 °C for 18 h. After blocking with the StartingBlock™ blocking buffer (Thermo Fisher Scientific) and being washing with PBS containing 0.01% Tween-20 (PBST) three times, the samples were added to the plates and incubated for 1 h at 37 °C. After washing, the plates were incubated with horseradish peroxidase-conjugated antihuman lambda light chain antibody (Bethyl Laboratories, Inc., Montgomery, TX, USA) for 1 h at RT, followed by washing with PBST. 3,3′,5,5′-Tetramethylbenzidine was subsequently added to induce the color reaction. After the reaction was stopped with 1 N HCl, the absorbance was read at 450 nm on a microplate reader; all measurements were performed in duplicate.

2.12. Surface plasmon resonance

The binding kinetics of QBEND/10 antibodies to CD34 (Fc tag; Sino Biological Incorporation) were measured using the Biacore system (Biacore X, GE Healthcare) in the running buffer HBS-EP (10 mM HEPES, pH 7.4; 150 mM NaCl; 3 mM EDTA; 0.005% surfactant P20). In brief, CD34 was immobilized onto a CM5 sensor chip through amine coupling to a level of 1200 response units, and purified antibodies of different concentrations were injected at a flow rate of 30 μL/min. The surface was regenerated by injecting 15 μL of 10 mM glycine–HCl, pH 2.5. Sensorgrams were obtained at each concentration and were evaluated using the BIA Evaluation 3.2 program (GE Healthcare). Binding data were fitted with a 2:1 (bivalent) binding model to calculate the affinity constant K_D, which was defined as the ratio of the dissociation rate (k_{off})/association rate (k_{on}).

2.13. Cell culture

HUVECs were obtained from the American Type Cell Culture (Manassas, VA, USA). For expansion, the cells were grown in an endothelial cell medium (ECM) supplemented with 5% FBS, 1% endothelial cell growth supplement (ECGS), and 1% penicillin/streptomycin (5% CO_2 at 37 °C). ECM, ECGS, and antibiotics were obtained from ScienCell Research Laboratory. HUVECs were used between passage 7 and 9.

2.14. Tube formation assay

HUVECs were pretreated with $VEGF_{165}$ (25 ng/mL, Sigma–Aldrich) in the presence or absence of anti-VEGF IgG (G6-31) [45] in starvation medium (ECM containing 1% FBS) at 37 °C in a humidified atmosphere of 5% CO2 for 24 h. The tube formation assay was performed using growth factor-reduced Matrigel (BD Biosciences) added to 15-well microslides (Ibidi, Germany); the gel was allowed to solidify at 37 °C for 1 h. Subsequently, subconfluent HUVECs were prestained with 10 μg/mL $DiIC_{12}(3)$ fluorescent dye (BD Biosciences) at 37 °C for 1 h and then harvested with trypsin–EDTA. To evaluate the effects of mouse or humanized QBEND/10, HUVECs were resuspended in starvation medium in the presence or absence of QBEND/10 antibodies at various concentrations and then seeded onto the Matrigel layer at a cell density of 8×10E3 cells per well. After 18 h of incubation, tubular network structures were visualized and photographed using an inverted fluorescence microscope. Cell-covered area and junctions were quantified using ImageJ software.

2.15. Flow cytometry analysis

HUVECs were harvested with trypsin–EDTA. All immunofluorescent labeling and washing was performed in Stain Buffer (BSA) (BD Biosciences). Cells were incubated with an irrelevant isotype control or the mouse antihuman CD34 antibody (5 μg/mL, QBEND/10) for 1 h at 4 °C. After 3 times washing with cold Stain Buffer, FITC-conjugated goat antimouse IgG (1:100, Jackson ImmunoResearch) were added to the cells for 45 min in the dark at 4 °C, followed by washing. Flow cytometry analysis was performed using a FACSCalibur system (BD Biosciences) in combination with CellQuest software (BD Biosciences).

3. Results

3.1. De novo protein sequencing of variable fragments of mouse QBEND/10

LC–MS/MS-based techniques have emerged as a crucial tool for

protein identification [46–48]. Detailed information on peptide sequences can be obtained by assigning fragment ions provided by MS/MS spectra. At present, Mascot is the most popular search engine, and its probability-based scoring algorithm has been widely used. Higher Mascot scores usually increases the confidence on peptide assignment for de novo sequencing. To achieve greater sequence coverage, in-solution digestion by using several enzymes and in-gel digestion with trypsin for the separated heavy and light chains were performed. LC–MS/MS was used to analyze all the resulting peptides, and peak lists were generated for an iterative database search and an error-tolerant search against customized databases. Only the peptides with high-quality MS/MS spectra (ion score, ≥30) were listed. The theoretical tryptic peptides for the QBEND/10 VL and VH segments are listed in Tables 1 and 2. The base peak intensity chromatograms of the QBEND/10 light and heavy chains digested by trypsin are shown in Fig. 1A and B. Ln and Hn indicate the nth tryptic peptide assigned from the N-terminal of the light and heavy chains, respectively. Each peak was identified and assigned according to the data in Tables 1 and 2. The identification results of the VL and VH segments from multiple enzyme digestion are aligned and shown in Fig. 2A and B.

Table 1
Theoretical peptides of QBEND/10 light chains obtained using trypsin digestion.

Theoretical M.W.	Peptide no.	Amino acid no.	Sequence
1880.9843	L1	1–19	QLVLTQSSSASFSLGASAK
1144.5659	L2	20–29	LTCTLSSQHR
2003.0516	L3	30–45	TFTIEWYQQQPLKPPK
809.4105	L4	46–51	YVMELR
146.1055	L5	52–52	K
1312.5643	L6	53–65	DGSHSTGDGIPDR
969.4152	L7	66–75	FSGSSSGADR
2639.3152	L8	76–99	YLSISNIQPEDEAIYICGVG NTIK
1330.6557	L9	100–111	EQFVYVFGGGTK
840.5069	L10	112–119	VTVLGQPK
1731.8930	L11	120–135	STPTLTVFPPSSEELK
389.1910	L12	136–138	ENK
2092.1027	L13	139–158	ATLVCLISNFSPSGVTVAWK
1699.8377	L14	159–175	ANGTPITQGVDTSNPTK
446.2125	L15	176–179	EGNK
1824.8617	L16	180–194	FMASSFLHLTSDQWR
2017.8799	L17	195–212	SHNSFTCQVTHEGDTVEK
818.3844	L18	213–220	SLSPAECL

3.2. Molecular modeling of QBEND/10

Molecular modeling of mouse QBEND/10 was performed using PIGS [35,36], as described in Materials and Methods. The final refined 3D structure of the Fv region was viewed using the Swiss-PdbViewer (DeepView) application [40] (Fig. 3). Both VL and VH fragments of mouse QBEND/10 were modeled using the most accurate matches with the highest sequence identities of known templates from different structures. The PDB codes of the templates for mouse QBEND/10 Fv regions are as follows (sequence identity is indicated in parentheses): 2GKI [37] for the heavy chain (86.67%) and 2QHR [38] for the light chain (94.92%); 2QHR for CDR-L1 (75%), CDR-L2 (85.71%), and CDR-L3 (92.31%) and 2GKI for CDR-H1 (90%), CDR-H2 (82.35%), and CDR-H3 (45.45%). All CDRs were modeled on the basis of canonical conformations defined for those particular canonical structure classes.

3.3. Humanization of QBEND/10

Through NCBI IgBLAST, the human germline V region from the IGHV1–3*01 and IGLV4–69*01 groups showed the highest identity to

Table 2
Theoretical peptides of QBEND/10 heavy chains obtained using trypsin digestion.

Theoretical M.W.	Peptide no.	Amino acid no.	Sequence
1993.0844	H1	1–19	QVQLEQSGPELVKPGASVK
467.1872	H2	20–23	MSCK
1757.8777	H3	24–38	ASGYTFTSYVIHWVK
2407.1808	H4	39–59	QKPGQGLEWLGYTNPYNDVTK
552.2544	H5	60–63	YNEK
293.1739	H6	64–65	FK
293.1739	H7	66–67	FK
734.3810	H8	68–74	ATLTSDK
2709.1574	H9	75–98	QSTTAYMEFSSLTSEDSAVYYCAR
2639.2366	H10	99–122	YGGLWLYAMDYWGQGTSVTVSSAK
2802.4295	H11	123–150	TTPPSVYPLAPGSAAQTNSMVTLGCLVK
6497.1325	H12	151–212	GYFPEPVTVTWNSGSLSSGVHTFPAVLQSDLYTLSSSVTVPSSTWPSETVTCNVAHPASSTK
360.2009	H13	213–215	VDK
146.1055	H14	216–216	K
483.3169	H15	217–220	IVPR
2693.3089	H16	221–245	DCGCKPCICTVPEVSSVFIFPPKPK
1099.6488	H17	246–255	DVLTITLTPK
1061.5791	H18	256–265	VTCVVVDISK
2844.2990	H19	266–289	DDPEVQFSWFVDDVEVHTAQTQPR
1156.5149	H20	290–298	EEQFNSTFR
1852.9141	H21	299–314	SVSELPIMHQDWLNGK
422.2165	H22	315–317	EFK
277.1209	H23	318–319	CR
1242.6608	H24	320–331	VNSAAFPAPIEK
447.2693	H25	332–335	TISK
247.1532	H26	336–337	TK
456.2808	H27	338–341	GRPK
1209.6757	H28	342–352	APQVYTIPPPK
605.2843	H29	353–357	EQMAK
261.1325	H30	358–359	DK
3574.6424	H31	360–389	VSLTCMITDFFPEDITVEWQWNAQPAENYK
1964.8826	H32	390–406	NTQPIMDTDGSYFVYSK
600.3595	H33	407–411	LNVQK
2847.2783	H34	412–436	SNWEAGNTFTCSVLHEGLHNHHTEK
811.4188	H35	437–444	SLSHSPGK

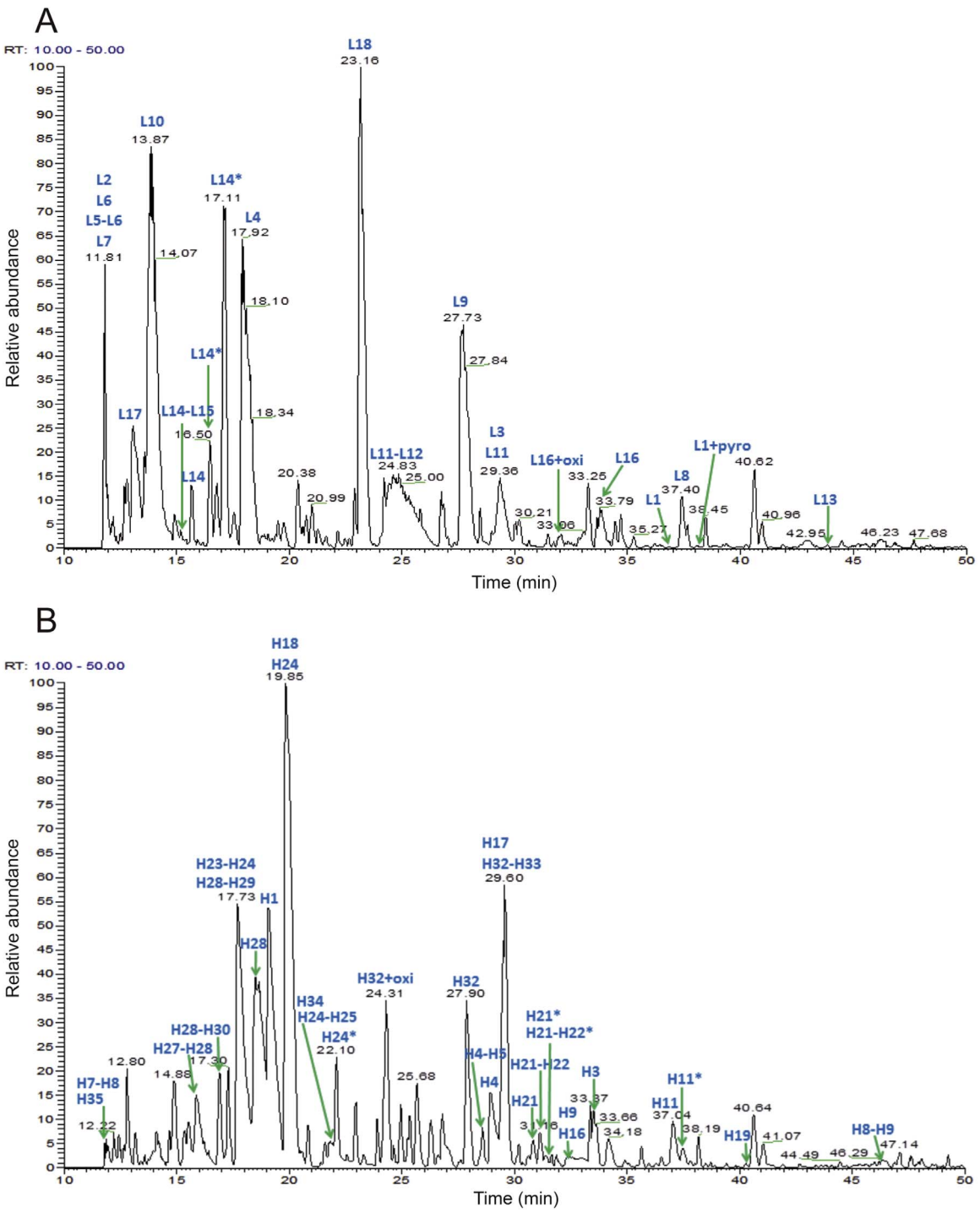

Fig. 1. BPI chromatogram of QBEND/10 light (A) and heavy (B) chains obtained using trypsin digestion. Ln and Hn denote the nth peptide counted from the N-terminal of QBEND/10 light and heavy chains, respectively. Stars indicate deamidated peptides. Pyro indicates pyroglutamate at Q, and oxi denotes oxidation at M.

mouse QBEND/10 VH (67.3%) and VL (70.1%), respectively. The sequence alignment of the mouse and human templates is shown in Fig. 4A and B. The J regions for the heavy (IGHJ4*01) and light (IGLJ1*01) chains were selected from the most identical human consensus sequences, which showed one mismatched residue each for VH (WGQGTSVTVSS) and VL (FGGGTKVTVLGQP). The QBEND/10 model (Fig. 3) was used to identify surface accessible residues. Twenty-eight amino acids in the VH of QBEND/10 (Fig. 4A) were identified as surface accessible residues. Excluding CDRs, only 4 (Gln5Val, Pro9Ala, Lys73Thr, and Gln74Ser) of the 28 amino acids differed from the human germline sequence and were adapted to the human version. Considering QBEND/10 VL (Fig. 4B), 5 (Ser8Pro, Leu41Glu, Thr54dLys, Asn77Ser, and Gly100Thr) of 35 surface accessible amino acids differed from the human germline and were substituted with their corresponding amino acids. The residue numbers were calculated according to the method stated by Kabat et al. [49].

3.4. Construction and expression of QBEND/10

In this study, two mammalian expression vectors, pSecTag2/Hygro

A

```
T+G             1 QLVLTQSSSA SFSLGASAKL TCTLSSQHRT FTIEWYQQQP LKPPKXXXXX XXDGSHSTGD
Trypsin         1 QLVLTQSSSA SFSLGASAKL TCTLSSQHRT FTIEWYQQQP LKPPKYVMEL RKDGSHSTGD
In-gel T        1 QLVLTQSSSA SFSLGASAKL TCTLSSQHRT FTIEWYQQQP LKPPKYVMEL RKDGSHSTGD
Glu-C           1 QLVLTQSSSA SFSLGASAKL TCTLSSQHRT FTIEXXXXXX XXXXXXXXXX XXXXXXXXXX
Chymotrypsin    1 QLVLTQSSSA SFSLGASAKL TCTLXXXXXX XXXXXQQQP LKPPKYVMEL RKDGSHSTGD
Thermolysin     1 QLVLTQSSSA SFSLGASAKX XXXLSSQHRT FTIEWYQQQP LKPPKYXXXL RKDGSHSTGD
Subtilin        1 QLVLTQSSSA SFSLGASAKL TCTLSSQHRT FTIEXXQQQP LKPPKYVXXX RKDGSHSTGD

T+G            61 GIPDRXXXXX XXXXXYLSIS NIQPEDEAIY ICGVGNTIKE QFVYVFGGGT KVTVLGQPKS
Trypsin        61 GIPDRFSGSS SGADRYLSIS NIQPEDEAIY ICGVGNTIKE QFVYVFGGGT KXXXXXXXXS
In-gel T       61 GIPDRFSGSS SGADRYLSIS NIQPEDEAIY ICGVGNTIKE QFVYVFGGGT KVTVLGQPKS
Glu-C          61 XXXXXXXXXX XXXXXXXXXX XXXXXDEAIY ICGVGNTIKE QFVYVFGGGT KVTVLGQPKS
Chymotrypsin   61 GIPDRFSGSS SGADRYLSIS NIQPEDEAIY ICGVGNTIKE QFVYXXXXXX XXXXXXXXXX
Thermolysin    61 GIPDRFSGSS SGADRYXXXX XXXXXXXXXX XXXXXXXXXX XXXXVFGGGT KVTVLGQPKS
Subtilin       61 GIPDRFSGSX XXXXXYLSIS NIQPEDEAIY ICGVGNTIKX XXXXXXXXXX XXXXXXXXXS
```

B

```
T+G             1 QVQLEQSGPE LVKPGASVKX XXXASGYTFT SYVIHWVKQK PGQGLEWLGY TNPYNDVTKX
Trypsin         1 QVQLEQSGPE LVKPGASVKX XXXXSGYTFT SYVIHWVKQK PGQGLEWLGY TNPYNDVTKY
In-gel T        1 QVQLEQSGPE LVKPGASVKM SCKASGYTFT SYVIHWVKQK PGQGLEWLGY TNPYNDVTKY
Glu-C           1 XXXXXXXXXX XXXXXXXXXX XXXXXXXXXX XXXXXXXXXX XXXXXXWLGY TNPYNDVTKY
Chymotrypsin    1 XXXXXXXXXX XXXXXXXXXX XXXXXXXXXX XXXXXXXXXX XXXXXXXXXX TNPYNDVTKY
Thermolysin     1 XXXXXXXXXX XXXXXXXXXX XXXXXXXXXX XXXXXXXXXX XXXXXXXLGY TNPYNDVTKY
Subtilin        1 XXXXXQSGPE LVKPGASXXX XXXASGYTFT SYVIHWVKXX XXXXXXXXXX XXXXXXXXXX

T+G            61 XXXXXXXXXX XXXXQSTTAY MEFSSLTSED SAVYYCARYG GLWLYAMDYW GQGTSVTVSS
Trypsin        61 NEKXXXXXXX XXXXQSTTAY MEFSSLTSED SAVYYCARYG GLWLYAMDYW GQGTSVTVSS
In-gel T       61 NEKXXFKATL TSDKQSTTAY MEFSSLTSED SAVYYCARYG GLWLYAMDYW GQGTSVTVSS
Glu-C          61 NEXXXXXXXX XXXXXXXXXX XXXXXXXXXX XXXXXXXXXX XXXXXXXXXX XXXXXXXXXX
Chymotrypsin   61 NEKFXXXXXX XXXXXXXXXX XXXXXXXXXX XXXXXXXXXX XXXXXXXXXX XXXXXXXXXX
Thermolysin    61 NEKXXXXXXX XXXXXXXXXX XXXXXLTSED SAVYYCARYG GLWXXXXXXX XXXXXXXXXX
Subtilin       61 XXXXXXXXXX XXXXQSTTAY MEFSSLTSED SAVYYCARYG GLWLYAMDYW GQGTSVTVSS
```

Fig. 2. Multiple enzyme digestion and in-gel digestion sequence alignment for QBEND/10 light (A) and heavy (B) chain variable regions.

and pcDNA3.3, were used to express the QBEND/10 IgG molecule as previously described by Chiu et al. [50]. To aid QBEND/10 secretion in culture media, a leader sequence was added upstream of the heavy and light chains, respectively. The amino acid sequences of QBEND/10 VH and VL were cloned in-frame with the human IgG gamma 1 heavy chain and lambda light chain constant regions, respectively. Chimeric and humanized QBEND/10 antibodies were expressed as soluble secretory proteins in mouse myeloma NS0 cells. Each culture medium was purified using IgSelect (GE Healthcare) and analyzed though SDS-PAGE. As shown in Fig. 5, one prominent band of approximately 150 kDa in nonreducing conditions and two clear bands of approximately 50 kDa (heavy chain) and approximately 25 kDa (light chain) in reducing conditions were observed.

3.5. Antibody binding analysis

The binding affinities of two antibodies, chimeric and humanized QBEND/10, with recombinant CD34 were determined using a surface plasmon resonance biosensor-based assay, and the binding kinetics were determined. The K_D of the binding of chimeric QBEND/10 with CD34 was 14.7 nM, whereas that of the humanized QBEND/10 with the CD34 protein was 7.34 nM (Table 3). In both instances, the k_{off} was approximately 2.6×10E4 s^{-1}, whereas the k_{on} increased by two-fold for the humanized QBEND/10 (from 1.78×10E4 M^{-1} s^{-1} to 3.66×10E4 M^{-1} s^{-1}; Table 3). The similar K_D values of the chimeric and humanized QBEND/10 indicated that the process of humanization did not alter the binding affinity of CD34.

3.6. Effects of various culture conditions on CD34 expression

Previous data have shown that freshly isolated HUVECs are 90–95% $CD34^+$, but CD34 expression is rapidly lost when cells are cultured [13,51]. In this study, we kept HUVECs in culture (complete ECM) for a period of 7 days without being passaged, the proportion of $CD34^+$ cells strongly increased (39.62%) at passage 8 (Fig. 6A). Furthermore, stimulated the 7-day cultured HUVECs with serum starvation in the absence or presence of $VEGF_{165}$ (25 ng/mL) for 24 h showed a more increased percentage of $CD34^+$ HUVECs, 44.75% (Fig. 6B) and 60.82% (Fig. 6C), respectively.

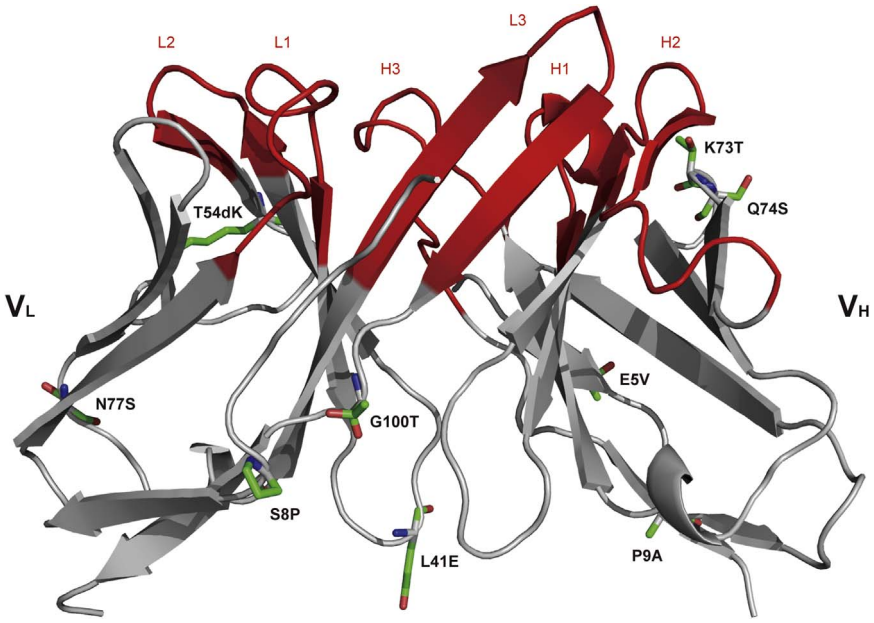

Fig. 3. Molecular model of the QBEND/10 variable regions. The 3D structure of the mouse QBEND/10 Fv region is generated using the Web-based antibody structure prediction program PIGS. Nine amino acids (in boldface), namely four and five residues in the VH and VL frameworks, respectively, are substituted with human germline residues. The CDR loops are shown in red.

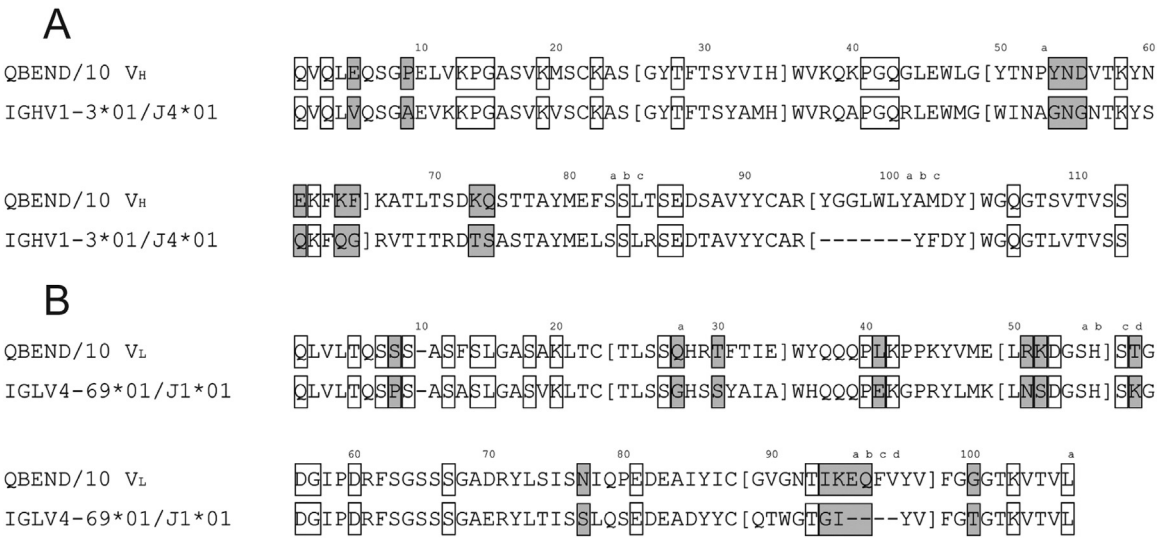

Fig. 4. Sequence alignment of mouse QBEND/10 with corresponding human germline sequence. The QBEND/10 heavy (A) and light (B) chain variable regions are sequence-aligned to the most homologous human germline genes IGHV1–3*01/J4*01 and IGLV4–69*01/J1*01, respectively. The conserved surface residues are marked with empty boxes, and the nonconserved surface residues are shown as shaded boxes. The CDRs (within brackets) are unchanged.

3.7. Effects of humanized QBEND/10 on VEGF$_{165}$-induced tube formation of endothelial cells

The HUVEC tube formation assay is an in vitro angiogenesis assay, which recapitulates some angiogenesis steps and has been used for many years [52,53]. HUVECs on the Matrigel formed tube-like structures (Fig. 7A). Cell-covered area and the number of junctions were calculated using ImageJ, which directly revealed the ability of the HUVECs to form capillary-like structures. As shown in Fig. 7B and C, VEGF$_{165}$ promoted tube formation, whereas the humanized QBEND/10 (10 μg/mL) or anti-VEGF IgG (10 μg/mL) significantly inhibited VEGF$_{165}$-dependent tube formation. These results demonstrated that the humanized QBEND/10 exhibited similar potential as anti-VEGF IgG in inhibiting VEGF$_{165}$-induced tube formation.

4. Discussion

Angiogenesis is a characteristic of cancer and contributes not only to tumor growth but also to tumor cell invasion [54]. Targeting tumor angiogenesis has focused on the VEGF pathway. Bevacizumab, the recombinant humanized VEGF-A-specific mAb, was approved by the U.S. Food and Drug Administration for treating brain, lung, kidney, ovarian, and colon cancers. Anti-VEGF therapy showed significant clinical benefits for treating some cancers but was not as efficacious as expected [55]. Moreover, a recent study focused on the tumor microenvironment as a possible source of resistance to anti-VEGF therapy [56]. The CD34 function in the tumor microenvironment was previously reported [11]. Anti-CD34 should be considered when developing combination therapies to overcome resistance to anti-VEGF therapy. In current study, we showed that QBEND/10 impairs the

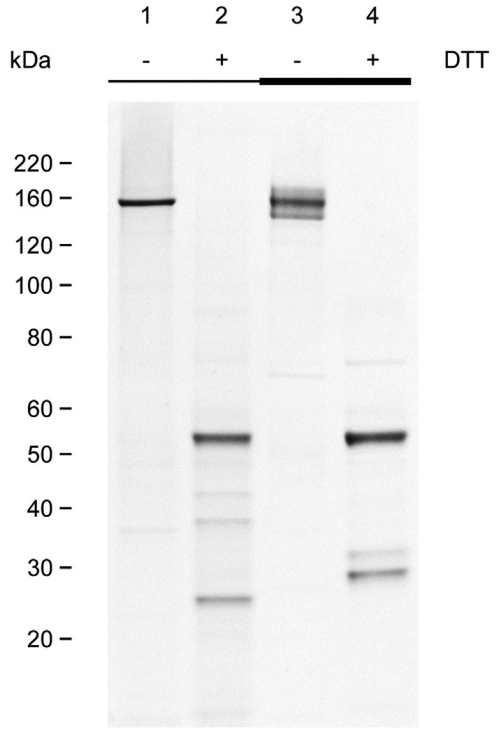

Fig. 5. Purification of chimeric and humanized QBEND/10 antibodies. The indicated chimeric QBEND/10 (lanes 1 and 2) and humanized QBEND/10 (lanes 3 and 4) antibodies were stably expressed in the mouse myeloma NS0 cells and purified from culture media by column chromatography. The samples were electrophoresed on a 4–12% NuPAGE Bis-Tris polyacrylamide gel with the MOPS buffer under nonreducing (lanes 1 and 3) and reducing (lanes 2 and 4) conditions. The gel was stained with Coomassie brilliant blue R-250.

Table 3
Binding kinetics of chimeric and humanized QBEND/10 to immobilized human CD34 protein.

Antibody	$k_{on}/10^4$ (M^{-1} s^{-1})	$k_{off}/10^{-4}$ (s^{-1})	K_D (nM)
Chimeric QBEND/10	1.78	2.62	14.7
Humanized QBEND/10	3.66	2.68	7.34

tube formation of human umbilical vein endothelial cells (HUVECs). Our finding is in accordance with the previous reports of that $CD34^{-/-}$ mice under some circumstances, exhibit an abnormal vessel morphology [10–12]. Moreover, $CD34^+$ HUVECs have been reported to show the antiangiogenic tip cell phenotype [31]. Therefore, CD34 could be a potential drug target for antiangiogenic therapy.

De novo sequencing remains challenging for large proteins such as mAbs, particularly because of its variable region, which cannot be searched in the existing database. In this study, multiple enzyme digestion was performed. Although trypsin provided the highest sequence coverage, the use of other enzymes, including thermolysin and subtilisin, enabled the identification of complementary sequences and confirmation of overlapping sequences. High-resolution MS facilitates obtaining more stringent criteria for database searching, which further increases the reliability of data interpretation.

Mouse QBEND/10 has been predominantly used in clinical experiments to isolate human stem cells [57,58]. It was classified as binding to the class II epitope of CD34 [34]. The recombinant QBEND/10 IgG has not been reported to date. Because the hybridoma cells of QBEND/10 were unavailable, we adopted the de novo protein sequencing approach to determine the amino acid sequences of the VH and VL of QBEND/10 IgG. By combining the de novo MS/MS sequencing and homologous database search, we successfully assembled the mouse mAb QBEND/10. In this study, the PIGS Web server was used for predicting and generating antibody homology models. Mouse QBEND/10 was subsequently humanized through variable domain resurfacing to minimize its immunogenicity. Humanized QBEND/10 can maintain the binding affinity and specificity of parental antibodies as well as impair the tube formation of HUVECs in vitro. Therefore, our humanization approach can provide a basis for developing a mAb for therapeutic use.

5. Conclusions

In conclusion, we provide a method to resolve the primary structure of the VH and VL of a mouse monoclonal antibody through de novo protein sequencing when hybridoma cells were unavailable. In addition, our humanization approach can conduct a basis for the development of monoclonal antibodies for therapeutic use and the humanized antibody can retain the binding affinity similar to that of the parental antibody.

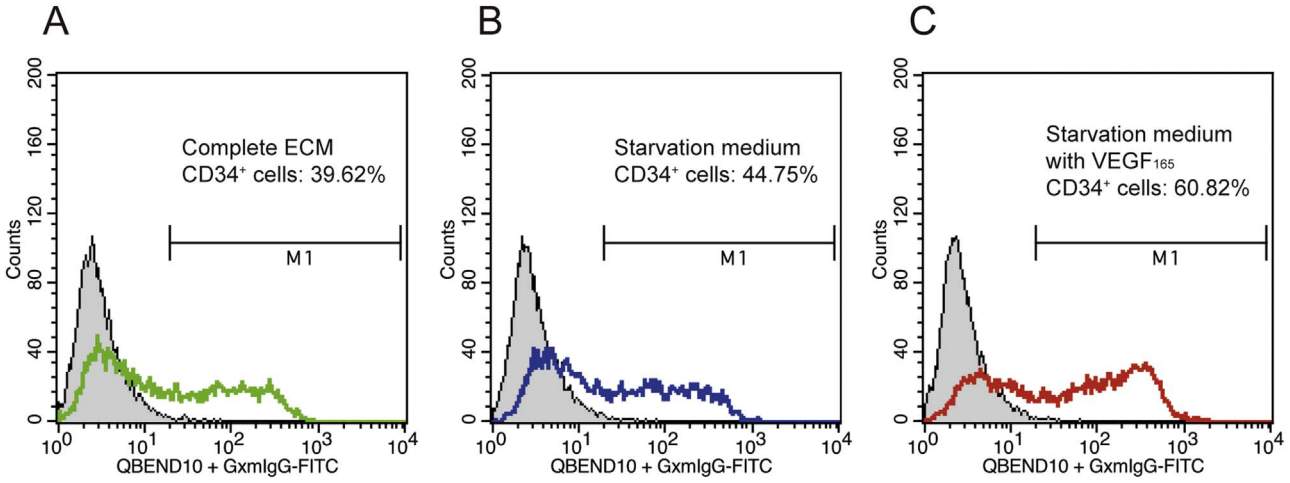

Fig. 6. The proportion of $CD34^+$HUVECs in different culture conditions. The proportion of $CD34^+$ cells was determined by flow cytometry after 7-day culturing. (A) Cells incubated with complete medium for 24 h. (B) Cells incubated with starvation medium for 24 h. (C) Cells stimulated with $VEGF_{165}$ in starvation medium for 24 h.

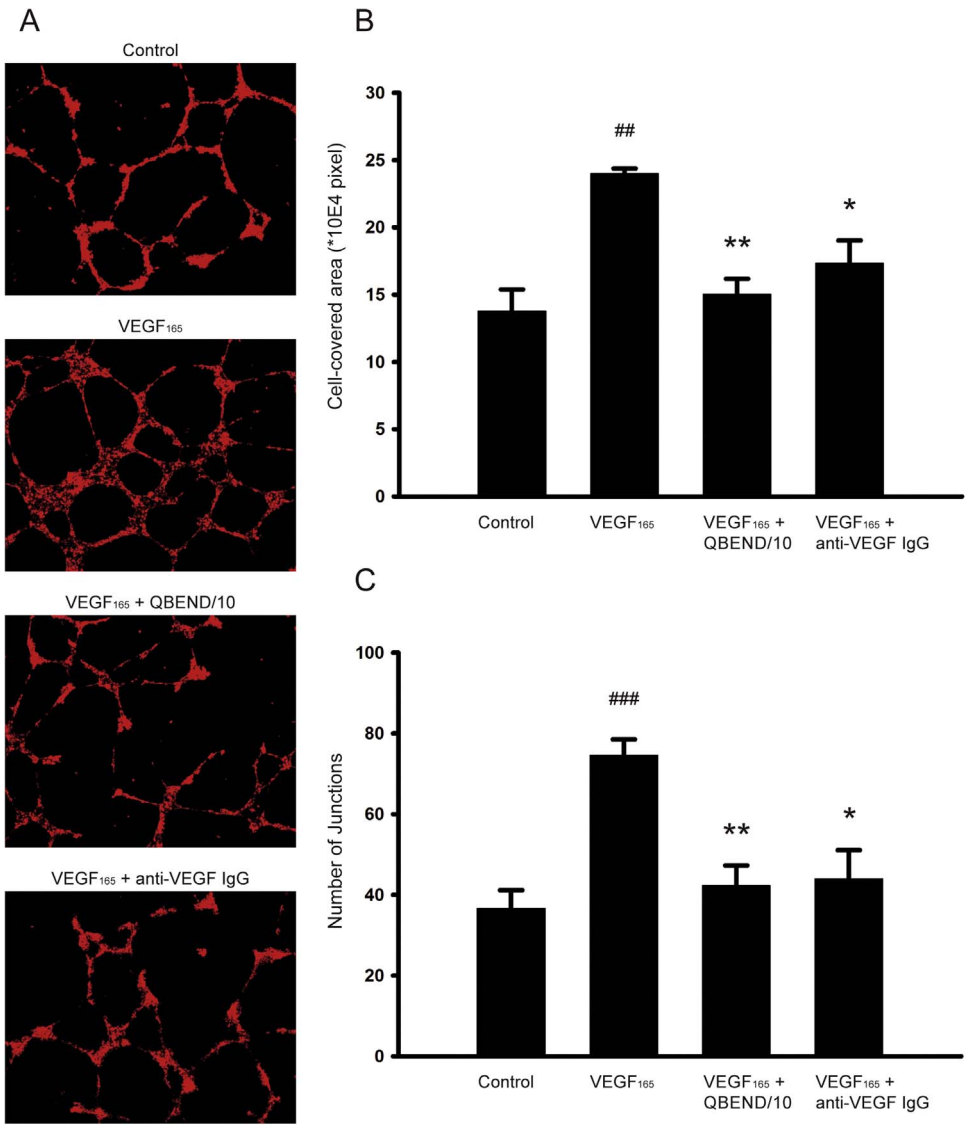

Fig. 7. Effects of the humanized QBEND/10 on $VEGF_{165}$-induced tube formation of human umbilical vascular endothelial cells. (A) Representative fluorescent images showing the inhibitory effect of humanized QBEND/10 on $VEGF_{165}$-induced HUVEC tube formation. HUVECs were treated with $VEGF_{165}$ (25 ng/mL) in the presence or absence of humanized QBEND/10 (10 μg/mL) or anti-VEGF IgG (10 μg/mL). (B, C) Capillary tube formation was quantified by counting the cell-covered area and junctions per field from A. One field was examined per well, with five wells per dose per experiment. Each column represents the mean ± standard error of the mean. $^{\#\#}P < 0.01$ and $^{\#\#\#}P < 0.001$ compared with the control group; $^{*}P < 0.05$ and $^{**}P < 0.01$ compared with the $VEGF_{165}$ group.

Acknowledgments

This work was funded by the Ministry of Economic Affairs, Grant numbers C356E13700 and E356EQ1100 (http://www.moeaidb.gov.tw/). The funders had no role in study design, data collection and analysis, decision to publish, or preparation of the manuscript.

We appreciate the structural bioinformatics service provided by the TMBD Bioinformatics Core (http//www.tbi.org.tw), funded by National Core Facility Program for Biotechnology, MOST 104–2319-B-400-002.

We are grateful to Hsiang-Ching Wang, Li-Tsen Lin and Si-Yuan Wu for the production of anti-VEGF IgG (G6-31).

Appendix A. Transparency document

Transparency document associated with this article can be found in the online version at http://dx.doi.org/10.1016/j.bbrep.2016.11.006.

References

[1] D.L. Simmons, A.B. Satterthwaite, D.G. Tenen, B. Seed, Molecular cloning of a cDNA encoding CD34, a sialomucin of human hematopoietic stem cells, J. Immunol. 148 (1) (1992) 267–271.

[2] J.S. Nielsen, K.M. McNagny, Novel functions of the CD34 family, J. Cell Sci. 121 (Pt 22) (2008) 3683–3692.

[3] C.I. Civin, L.C. Strauss, C. Brovall, M.J. Fackler, J.F. Schwartz, J.H. Shaper, Antigenic analysis of hematopoiesis. III. A hematopoietic progenitor cell surface antigen defined by a monoclonal antibody raised against KG-1a cells, J. Immunol. 133 (1) (1984) 157–165.

[4] R.G. Andrews, J.W. Singer, I.D. Bernstein, Monoclonal antibody 12-8 recognizes a 115-kd molecule present on both unipotent and multipotent hematopoietic colony-forming cells and their precursors, Blood 67 (3) (1986) 842–845.

[5] D. Soligo, D. Delia, A. Oriani, G. Cattoretti, A. Orazi, V. Bertolli, et al., Identification of CD34+ cells in normal and pathological bone marrow biopsies by QBEND10 monoclonal antibody, Leukemia 5 (12) (1991) 1026–1030.

[6] A. Ito, S. Nomura, S. Hirota, J. Suda, T. Suda, Y. Kitamura, Enhanced expression of CD34 messenger RNA by developing endothelial cells of mice, Lab. Invest. 72 (5) (1995) 532–538.

[7] T. Asahara, T. Murohara, A. Sullivan, M. Silver, R. van der Zee, T. Li, et al.,

Isolation of putative progenitor endothelial cells for angiogenesis, Science 275 (5302) (1997) 964–967.
[8] R.J. Berenson, R.G. Andrews, W.I. Bensinger, D. Kalamasz, G. Knitter, C.D. Buckner, et al., Antigen CD34+ marrow cells engraft lethally irradiated baboons, J. Clin. Invest. 81 (3) (1988) 951–955.
[9] A.R. Mackie, D.W. Losordo, CD34-positive stem cells: in the treatment of heart and vascular disease in human beings, Tex. Heart Inst. J. 38 (5) (2011) 474–485.
[10] M.R. Blanchet, M. Gold, S. Maltby, J. Bennett, B. Petri, P. Kubes, et al., Loss of CD34 leads to exacerbated autoimmune arthritis through increased vascular permeability, J. Immunol. 184 (3) (2010) 1292–1299.
[11] S. Maltby, S. Freeman, M.J. Gold, J.H. Baker, A.I. Minchinton, M.R. Gold, et al., Opposing roles for CD34 in B16 melanoma tumor growth alter early stage vasculature and late stage immune cell infiltration, PLoS One 6 (4) (2011) e18160.
[12] M.J. Siemerink, M.R. Hughes, M.G. Dallinga, T. Gora, J. Cait, I.M. Vogels, et al., CD34 promotes pathological epi-retinal neovascularization in a mouse model of oxygen-induced retinopathy, PLoS One 11 (6) (2016) e0157902.
[13] M.J. Siemerink, I. Klaassen, I.M. Vogels, A.W. Griffioen, C.J. Van Noorden, R.O. Schlingemann, CD34 marks angiogenic tip cells in human vascular endothelial cell cultures, Angiogenesis 15 (1) (2012) 151–163.
[14] Y. Cao, J. Arbiser, R.J. D'Amato, P.A. D'Amore, D.E. Ingber, R. Kerbel, et al., Forty-year journey of angiogenesis translational research, Sci. Transl. Med. 3 (114) (2011) 114rv3.
[15] J. Folkman, Tumor angiogenesis: therapeutic implications, N. Engl. J. Med. 285 (21) (1971) 1182–1186.
[16] H. Gerhardt, M. Golding, M. Fruttiger, C. Ruhrberg, A. Lundkvist, A. Abramsson, et al., VEGF guides angiogenic sprouting utilizing endothelial tip cell filopodia, J. Cell Biol. 161 (6) (2003) 1163–1177.
[17] G. Bergers, D. Hanahan, Modes of resistance to anti-angiogenic therapy, Nat. Rev. Cancer 8 (8) (2008) 592–603.
[18] I. Barkefors, S. Le Jan, L. Jakobsson, E. Hejll, G. Carlson, H. Johansson, et al., Endothelial cell migration in stable gradients of vascular endothelial growth factor A and fibroblast growth factor 2: effects on chemotaxis and chemokinesis, J. Biol. Chem. 283 (20) (2008) 13905–13912.
[19] P. Carmeliet, L. Moons, A. Luttun, V. Vincenti, V. Compernolle, M. De Mol, et al., Synergism between vascular endothelial growth factor and placental growth factor contributes to angiogenesis and plasma extravasation in pathological conditions, Nat. Med. 7 (5) (2001) 575–583.
[20] M. Autiero, A. Luttun, M. Tjwa, P. Carmeliet, Placental growth factor and its receptor, vascular endothelial growth factor receptor-1: novel targets for stimulation of ischemic tissue revascularization and inhibition of angiogenic and inflammatory disorders, J. Thromb. Haemost. 1 (7) (2003) 1356–1370.
[21] M. Marx, R.A. Perlmutter, J.A. Madri, Modulation of platelet-derived growth factor receptor expression in microvascular endothelial cells during in vitro angiogenesis, J. Clin. Invest. 93 (1) (1994) 131–139.
[22] M. Ziche, D. Maglione, D. Ribatti, L. Morbidelli, C.T. Lago, M. Battisti, et al., Placenta growth factor-1 is chemotactic, mitogenic, and angiogenic, Lab. Invest. 76 (4) (1997) 517–531.
[23] M. Zhou, R.L. Sutliff, R.J. Paul, J.N. Lorenz, J.B. Hoying, C.C. Haudenschild, et al., Fibroblast growth factor 2 control of vascular tone, Nat. Med. 4 (2) (1998) 201–207.
[24] D.J. Brat, A.C. Bellail, E.G. Van Meir, The role of interleukin-8 and its receptors in gliomagenesis and tumoral angiogenesis, Neuro Oncol. 7 (2) (2005) 122–133.
[25] A.E. Koch, P.J. Polverini, S.L. Kunkel, L.A. Harlow, L.A. DiPietro, V.M. Elner, et al., Interleukin-8 as a macrophage-derived mediator of angiogenesis, Science. 258 (5089) (1992) 1798–1801.
[26] A.B. Roberts, M.B. Sporn, R.K. Assoian, J.M. Smith, N.S. Roche, L.M. Wakefield, et al., Transforming growth factor type beta: rapid induction of fibrosis and angiogenesis in vivo and stimulation of collagen formation in vitro, Proc. Natl. Acad. Sci. USA 83 (12) (1986) 4167–4171.
[27] M.S. Pepper, Transforming growth factor-beta: vasculogenesis, angiogenesis, and vessel wall integrity, Cytokine Growth Factor Rev. 8 (1) (1997) 21–43.
[28] E.Y. Yang, H.L. Moses, Transforming growth factor beta 1-induced changes in cell migration, proliferation, and angiogenesis in the chicken chorioallantoic membrane, J. Cell Biol. 111 (2) (1990) 731–741.
[29] J. Holash, S.J. Wiegand, G.D. Yancopoulos, New model of tumor angiogenesis: dynamic balance between vessel regression and growth mediated by angiopoietins and VEGF, Oncogene 18 (38) (1999) 5356–5362.
[30] T.I. Koblizek, C. Weiss, G.D. Yancopoulos, U. Deutsch, W. Risau, Angiopoietin-1 induces sprouting angiogenesis in vitro, Curr. Biol. 8 (9) (1998) 529–532.
[31] C. Sgro, Side-effects of a monoclonal antibody, muromonab CD3/orthoclone OKT3: bibliographic review, Toxicology 105 (1) (1995) 23–29.
[32] W.Y. Hwang, J. Foote, Immunogenicity of engineered antibodies, Methods 36 (1) (2005) 3–10.
[33] M. Clark, Antibody humanization: a case of the 'Emperor's new clothes'?, Immunol. Today 21 (8) (2000) 397–402.
[34] M.W. Dercksen, D.G.M. de Haas, A.E.G. von dem Borne, C.E. van der Schoot, M10. 2 Characterization of the CD34 cluster. In: S.F. Schlossman, L. Boumsell, W. Gilks, J.M. Harlan, T. Kishimoto, C. Morimoto, et al. (Eds), Leucocyte typing V. White cell differentiation antigens, Proceedings of the 5th International Workshop and Conference, 1993 November 3–7, Boston, USA Oxford, New York, Oxford University Press, Tokyo, 1995, pp. 850–853.
[35] P. Marcatili, A. Rosi, A. Tramontano, PIGS: automatic prediction of antibody structures, Bioinformatics 24 (17) (2008) 1953–1954.
[36] P. Marcatili, P.P. Olimpieri, A. Chailyan, A. Tramontano, Antibody structural modeling with prediction of immunoglobulin structure (PIGS), Nat. Protoc. 9 (12) (2014) 2771–2783.
[37] Y.R. Kim, J.S. Kim, S.H. Lee, W.R. Lee, J.N. Sohn, Y.C. Chung, et al., Heavy and light chain variable single domains of an anti-DNA binding antibody hydrolyze both double- and single-stranded DNAs without sequence specificity, J. Biol. Chem. 281 (22) (2006) 15287–15295.
[38] J.E. Lee, A. Kuehne, D.M. Abelson, M.L. Fusco, M.K. Hart, E.O. Saphire, Complex of a protective antibody with its Ebola virus GP peptide epitope: unusual features of a V lambda x light chain, J. Mol. Biol. 375 (1) (2008) 202–216.
[39] G.G. Krivov, M.V. Shapovalov, R.L. Dunbrack Jr., Improved prediction of protein side-chain conformations with SCWRL4, Proteins 77 (4) (2009) 778–795.
[40] N. Guex, M.C. Peitsch, SWISS-MODEL and the Swiss-PdbViewer: an environment for comparative protein modeling, Electrophoresis 18 (15) (1997) 2714–2723.
[41] E.A. Padlan, A possible procedure for reducing the immunogenicity of antibody variable domains while preserving their ligand-binding properties, Mol. Immunol. 28 (4–5) (1991) 489–498.
[42] E.A. Kabat, National Institutes of H, U. Columbia, Sequences of proteins of immunological interest, U.S. Dept. of Health and Human Services, Bethesda, MD, Public Health Service, National Institutes of Health, 1991.
[43] J.T. Pedersen, A.H. Henry, S.J. Searle, B.C. Guild, M. Roguska, A.R. Rees, Comparison of surface accessible residues in human and murine immunoglobulin Fv domains. Implication for humanization of murine antibodies, J. Mol. Biol. 235 (3) (1994) 959–973.
[44] M.M. Bradford, A rapid and sensitive method for the quantitation of microgram quantities of protein utilizing the principle of protein-dye binding, Anal. Biochem. 72 (1976) 248–254.
[45] W.C. Liang, X. Wu, F.V. Peale, C.V. Lee, Y.G. Meng, J. Gutierrez, et al., Cross-species vascular endothelial growth factor (VEGF)-blocking antibodies completely inhibit the growth of human tumor xenografts and measure the contribution of stromal VEGF, J. Biol. Chem. 281 (2) (2006) 951–961.
[46] J.V. Olsen, B. Macek, O. Lange, A. Makarov, S. Horning, M. Mann, Higher-energy C-trap dissociation for peptide modification analysis, Nat. Methods 4 (9) (2007) 709–712.
[47] J.E. Syka, J.J. Coon, M.J. Schroeder, J. Shabanowitz, D.F. Hunt, Peptide and protein sequence analysis by electron transfer dissociation mass spectrometry, Proc. Natl. Acad. Sci. USA 101 (26) (2004) 9528–9533.
[48] A. Guthals, N. Bandeira, Peptide identification by tandem mass spectrometry with alternate fragmentation modes, Mol. Cell. Proteomics 11 (9) (2012) 550–557.
[49] E.A. Kabat, T.T. Wu, H. Bilofsky, M. Reid-Miller, H. Perry. Sequence of Proteins of Immunological Interest, National Institutes of Health, Bethesda, 1983.
[50] W.C. Chiu, Y.P. Lai, M.Y. Chou, Humanization and characterization of an anti-human TNF-alpha murine monoclonal antibody, PLoS One 6 (1) (2011) e16373.
[51] D. Delia, M.G. Lampugnani, M. Resnati, E. Dejana, A. Aiello, E. Fontanella, et al., CD34 expression is regulated reciprocally with adhesion molecules in vascular endothelial cells in vitro, Blood 81 (4) (1993) 1001–1008.
[52] Y. Kubota, H.K. Kleinman, G.R. Martin, T.J. Lawley, Role of laminin and basement membrane in the morphological differentiation of human endothelial cells into capillary-like structures, J. Cell Biol. 107 (4) (1988) 1589–1598.
[53] I. Arnaoutova, J. George, H.K. Kleinman, G. Benton, The endothelial cell tube formation assay on basement membrane turns 20: state of the science and the art, Angiogenesis 12 (3) (2009) 267–274.
[54] J. Folkman, What is the evidence that tumors are angiogenesis dependent?, J. Natl. Cancer Inst. 82 (1) (1990) 4–6.
[55] R.N. Eskander, L.M. Randall, Bevacizumab in the treatment of ovarian cancer, Biologics 5 (2011) 1–5.
[56] N. Ferrara, Pathways mediating VEGF-independent tumor angiogenesis, Cytokine Growth Factor Rev. 21 (1) (2010) 21–26.
[57] K. Kato, A. Radbruch, Isolation and characterization of CD34+ hematopoietic stem cells from human peripheral blood by high-gradient magnetic cell sorting, Cytometry 14 (4) (1993) 384–392.
[58] T.E. Thomas, P.M. Lansdorp, Purification of CD34 positive cells from human bone marrow using high gradient magnetic separation, Prog. Clin. Biol. Res. 377 (1992) 537–544.